Applied Catalysis B: Environmental 231 (2018) 191–199

Contents lists available at ScienceDirect

Applied Catalysis B: Environmental

journal homepage: www.elsevier.com/locate/apcatb

Direct electrolysis of waste newspaper for sustainable hydrogen production: an oxygen-functionalized porous carbon anode

Takashi Hibino[a,*], Kazuyo Kobayashi[a], Masaya Ito[a], Masahiro Nagao[a], Mai Fukui[b], Shinya Teranishi[b]

[a] Graduate School of Environmental Studies, Nagoya University, Nagoya, 464-8601, Japan
[b] Soken Inc., Nishio, Aichi 445-0012, Japan

ARTICLE INFO

Keywords:
Biomass electrolysis
Hydrogen production
Carbon anode
Newspaper

ABSTRACT

Biomass electrolysis enables hydrogen (H_2) production at onset voltages of less than 1 V, depending on the fuel species. However, biofuel derived from biomass not categorized as food and produced from environmentally friendly processes is needed for the development of sustainable strategies. In addition, the biofuel should not require special and expensive procedures for processing. The present report describes the direct electrolysis of waste newspaper for H_2 production. Cellulose and lignin included in the newspaper were subject to dissolution and hydrolysis in a phosphoric acid solvent at the anode in a temperature range of 100–175 °C. The resulting decomposition products were electrolyzed to H_2 and carbon dioxide (CO_2), at low onset voltages (*ca.* 0.2 V) and high current efficiencies (H_2: 1.0, CO_2: 0.9). Carbon black functionalized with carbonyl groups showed greater catalytic activity than a Pt/C catalyst for the anode reaction. H_2 yield reached *ca.* 0.2 g per 1 g of newspaper in a batch cell. H_2 was produced continuously in a current-density range of 0.15–0.25 A cm^{-2} while maintaining plateau-like voltage behavior in a flow cell. The energy consumed for electrolysis at a current density of 0.15 A cm^{-2} was as low as 1.27 kWh $(Nm^3)^{-1}$.

1. Introduction

Hydrogen (H_2) can be produced from water, biomass, natural gas, or coal [1]. Woody or herbaceous biomass is one of the most abundant and sustainable feedstocks. Unlike sugar- or starch-based crops, wood and grass raw materials are not used as food for human consumption [2]. Perennial weeds, paper waste, and wood chips have received attention as important feedstocks for H_2 production, because they are inexpensive and readily available [3]. Two conventional processes to convert woody and herbaceous biomass to H_2 have been developed: gasification [4,5] and fermentation [6,7]. Gasification involves partial oxidation with air or reforming with steam or carbon dioxide (CO_2). Critical technical issues include the large amount of nitrogen in the air, which lowers the H_2 content in the products, and the steam or CO_2 that requires an external heat supply for the endothermic gasification reactions. Biological H_2 production involves three major steps: raw material pretreatment, cellulose hydrolysis, and glucose fermentation. The pretreatment is required to remove lignin from the raw material and to reduce the crystallinity of cellulose. Enzymatic hydrolysis must be performed under precise enzyme control, while catalytic hydrolysis requires treatment of downstream wastes. For both gasification and fermentation, the separation and purification of H_2 add to the cost of the hydrogen [8]. These drawbacks limit the utilization of biomass as a biofuel for H_2 production.

One approach to achieving low-cost and highly efficient biomass H_2 production is to electrolyze biomass wastes effectively to H_2 in one step. Pioneering works in this field indicated that bioethanol electrolysis enabled H_2 production at an onset voltage lower than 1 V through the following reactions [9–11]:

$$C_2H_5OH + 3H_2O \rightarrow 2CO_2 + 12H^+ + 12e^- \quad (1)$$

$$12H^+ + 12e^- \rightarrow 6H_2 \quad (2)$$

As a result, pure H_2 is generated without requiring a separation process. However, this technology has limitations inherent in the fermentation of saccharides. In addition, this process has the disadvantage of leaving high-calorie lignin unused.

Similar anode reactions have been demonstrated for cellulose [12,13] and lignin [14]:

$$C_{6n}H_{10n+2}O_{5n+1} + (7n\text{-}1)H_2O \rightarrow 6nCO_2 + 24nH^+ + 24ne^- \quad (3)$$

$$(C_{31}H_{34}O_{11})_n + 51nH_2O \rightarrow 31nCO_2 + 136nH^+ + 136ne^- \quad (4)$$

* Corresponding author.
E-mail address: hibino@urban.env.nagoya-u.ac.jp (T. Hibino).

https://doi.org/10.1016/j.apcatb.2018.03.021
Received 30 November 2017; Received in revised form 8 February 2018; Accepted 7 March 2018
Available online 08 March 2018
0926-3373/

Note that Reactions (3) and (4) represent the results of several intermediate steps at the anode, including dissolution of the cellulose and lignin in phosphoric acid (H_3PO_4), their degradation, and charge-transfer reactions of the degraded products. For lignin, the anode and cathode reactions began at cell voltages greater than 0.3 V, with high current efficiencies of approximately 1.0 for H_2 production at the cathode and approximately 0.85 for CO_2 production at the anode. The operation temperature was in the range of 100–175 °C, which is thermally self-sustainable, due to the heat generated by the internal resistance of the cell [15].

Biomass wastes are lignocellulosic materials that possess more complex structures and higher molecular weights than pure cellulose and lignin, leading to lower solubility of cellulose and lignin in the H_3PO_4 solvent. Furthermore, Reactions (3) and (4) were achieved using a Pt/C anode, which is expensive and easily anodically corroded. Newspaper is made through a thermomechanical pulping process that does not remove lignin, unlike chemical pulping processes. In the present study, an attempt was made to electrolyze waste newspaper directly to H_2 using a Pt-free anode by functionalizing a porous carbon electrode. Acid functional groups, especially carbonyl groups, have redox activity due to the following equilibrium reaction [16,17]:

$$C = O + H^+ + e^- \rightleftharpoons C - OH \quad (5)$$

Carbon can be functionalized using physical, chemical, and electrochemical processes, as reviewed elsewhere [18–20]. Among these, acid treatment is one of the most useful techniques to modify the carbon surface because it causes less damage to the carbon structure than the other methods [21]. The goals of the present work include: (1) determining the best carbon black species as an alternative to a Pt/C anode, (2) modification of the carbon anode by surface oxygenation, (3) comparison of the electrolysis characteristics of the new anode with those of the Pt/C anode, (4) determining the H_2 yield per g of newspaper, (5) demonstrating continuous H_2 production, and (6) evaluating the recyclability of the H_3PO_4 solvent.

2. Experimental

2.1. Materials

A proton-conducting electrolyte membrane was prepared by mixing 1.0 g of $Sn_{0.9}In_{0.1}P_2O_7$ powder with 0.04 g of polytetrafluoroethylene (PTFE) powder, followed by cold-rolling the mixture to a thickness of 250 μm using a laboratory rolling mill. Details of the procedures have described previously [12–14]. Three types of carbon black (Vulcan XC-72R, Ketjen black EC-600JDK, and acetylene black) were purchased from Cabot, Akzo Nobel, and Denka, respectively. The Ketjen black was modified as follows [22]. The carbon (1.0 g) was stirred in 50 mL of 24% nitric acid (HNO_3) at room temperature for 0–74 h. After filtering and washing, the residual carbon was dried under vacuum at 120 °C for 6 h. The oxygenated carbon was subsequently heated at 800 °C for 5 h in a flow of 10% H_2 in an argon carrier. The unmodified, oxygenated, or partially reduced carbon was dispersed with a small amount of 85% H_3PO_4 (Wako Chemicals) in a mixer (Thinky AR-100) for 30 min. The slurry obtained was deposited on the surface of carbon fiber paper (Toray TGP-H-090). A commercially available Pt/C (Pt loading: 2 mg cm^{-2}, Electrochem) was used as a control anode and as the cathode. Printed and unprinted newspapers were supplied from Chunichi Shimbun Co., Ltd. The newspaper sample was cut into 2- to 4-mm pieces (for the batch operation) and pieces less than 1 mm (for the flow operation).

2.2. Characterization

Printed newspaper samples were characterized using the wood analytical method modified by Saka et al. [23], ^{13}C magic angle spinning (MAS) nuclear magnetic resonance (NMR), and gel permeation chromatography (GPC). Chemical composition of the samples was determined using the following procedures. To determine the moisture content, the sample was heated at 105 °C for 1 h and weighed after cooling to room temperature in a desiccator. To calculate the ash content, the dried sample was incinerated at 600 °C for 2 h. To determine the amounts of alcohol- and benzene-soluble content, dried samples were extracted in a Soxhlet extractor with a mixture of ethanol and benzene for 6 h and then with ethanol for 4 h. The degreased sample was reacted with 72% sulfuric acid (H_2SO_4) at room temperature for 1 h, followed by dilution to 3% H_2SO_4, heating in an autoclave at 120 °C for 1 h, and filtering to obtain the acid-insoluble lignin content. The content of acid-soluble lignin in the filtrate was determined from ultraviolet (UV) absorbance at 210 nm [24]. The degreased sample was also treated with sodium chlorite at 70–80 °C for 1 h and filtered to obtain holocellulose [23]. Cellulose was extracted from the holocellulose with 17.5% sodium hydroxide to give the cellulose content [25]. Hemicellulose content was calculated by the difference in weight between the holocellulose and cellulose content. The NMR analysis was conducted using a Bruker AVANCE 400 spectrometer (100 MHz). A cross polarization (CP) technique was used with ^1H decoupling during the ^{13}C NMR measurements. Molecular weight distribution profiles were obtained using a TRC GPC-10 chromatograph. Solvents used for cellulose and lignin were lithium chloride/N,N-dimethylacetamide and tetrahydrofuran (THF), respectively. Composition of the saccharide and aliphatic derivatives in the filtrate from the newspaper degraded with 85% H_3PO_4 was determined using high-performance liquid chromatography with tandem mass spectrometry (LC/MS; Shimadzu LC-30AD). The pore characteristics of the samples were determined by nitrogen adsorption at liquid nitrogen temperature (Bel Japan BELSORP18PLUS-HT). The specific surface area was calculated using the Brunauer-Emmett-Teller (BET) method from adsorption data in the relative pressure range of 0.001 to 0.3. The micro- and mesopore volume distributions were determined using the standard micropore method (MP) and the Barrett-Joyner-Halenda (BJH) method, respectively. Samples for adsorption measurements were pre-treated under vacuum at 200 °C for 30 min. The chemical charge state of C1s was analyzed using X-ray photoelectron spectroscopy (XPS; VG Escallab220i-XL). The quantities of H_2 and CO_2 evolved from the cathode and anode, respectively, were monitored using a mass spectrometer (MS; Pfeiffer Vacuum ThermoStar).

2.3. Electrochemical measurements

Batch and flow electrolysis systems were fabricated for the electrochemical measurements. The anode (area: 2.0 cm^2) and cathode (area: 0.5 cm^2) were used for both cells. The diameter of the electrolyte membrane was adjusted to 16 mm for the batch cell and 30 mm for the flow cell. In the batch cell, 15 mg of newspaper were impregnated with *ca.* 270 mg of 85% H_3PO_4, and the paste was deposited on the surface of the anode. The anode was attached to a stainless steel current collector (material: SUS316, diameter: 16 mm; Hohsen) and then sealed using a PTFE gasket (Nitto Denko) with PTFE tape (Nitto Denko). The cathode was supplied with argon at a flow rate of 100 mL min^{-1}. The batch cell was placed in an electric furnace (not illustrated) equipped with a thermocouple to provide feedback for temperature control (Fig. S1). The flow cell consisted of two different types of stainless-steel plates, a PTFE gasket, and the electrolysis cell. A liquid flow channel was created in the anode plate and connected with inlet and outlet tubes. A liquid mixture of newspaper and 85% H_3PO_4 (newspaper concentration: 0.35 wt%) was pumped to the anode at a flow rate of 0.44 mL min^{-1} using a syringe feeder. The cathode was supplied with argon in a manner similar to that of the batch cell. A pair of cartridge heaters, 40 mm in length and 5 mm in diameter, and a thermocouple with a diameter of 1 mm (not illustrated) were inserted into the anode plate (Fig. S1). The temperature of the batch and flow cells was monitored by

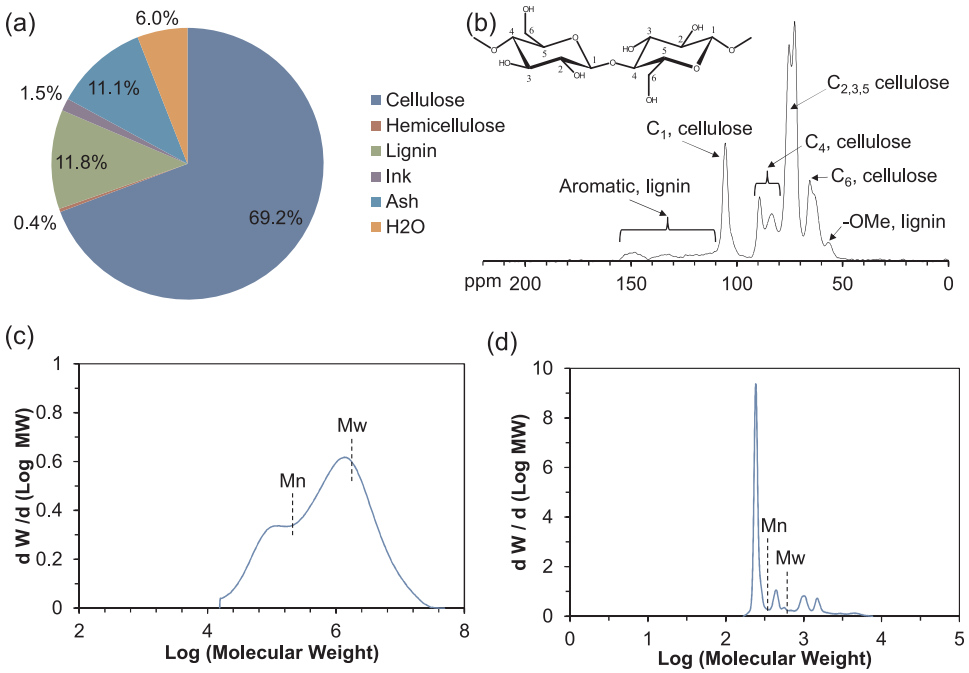

Fig. 1. Chemical characteristics of the newspaper: (a) chemical composition and (b) ^{13}C CP/MAS spectrum. Molecular weight distributions of (c) cellulose and (d) lignin included in the newspaper.

attaching a thermocouple to the cathode surface. Current-voltage (*I-V*) curves and impedance spectra were obtained using an electrochemical interface (Solartron 1287) and frequency response analyzer (Solartron 1260). The potentiostatic and galvanostatic measurements were performed at a scan rate of 20 mV sec^{-1} and in a current-density range of 0.06–0.30 A cm^{-2}, respectively. The impedance spectra were recorded at a bias voltage of 0.4 V in a frequency range of 0.1–10^6 Hz, unless otherwise stated. The current density was normalized using the area of the cathode.

3. Results and discussion

3.1. Chemical characteristics of newspaper

Fig. 1(a) shows the chemical composition of the newspaper used in the present study. This sample consisted of cellulose, hemicellulose, lignin, and ash that originated from the wood raw material, and small amounts of alcohol- and benzene-soluble components originating from the ink. Entezari et al. reported that the composition of newspaper is approximately the same as that of wood [26]. However, the lignin content in this sample (11.8%) was about half of that reported (20–27%), probably due to the difference in the production processes of the newspapers. Newspapers are produced by mixing thermo-mechanical pulp with the chemical pulp in a certain ratio [27]: hemicellulose as well as lignin are removed with sulfites in the chemical pulping process, which results in a low hemicellulose content, as shown in Fig. 1(a) (0.4%). Assuming that 15 mg of newspaper with this composition is electrolyzed to H_2 according to Reactions (3) and (4), the quantity of the H_2 produced is 2.4 mg. Fig. 1(b) shows the ^{13}C CP/MAS spectrum of the newspaper. Large, sharp signals recorded in a range of 65–105 ppm were assigned to cellulose C_{1-6} carbons [28]. Broad signals observed in the range of 110 – 160 ppm and a small signal appearing at 57 ppm were assigned to lignin aromatic hydrocarbons and methoxy groups, respectively [28]. Although the CP/MAS method does not provide a quantitative composition of the respective components, the newspaper likely was cellulose-rich, which is consistent with previously reported results [29]. Molecular weight distributions of cellulose and lignin in the newspaper are shown in Figs. 1(c) and (d), respectively. The weight-average molecular weight (Mw) and number-average molecular weight (Mn) of cellulose were determined to be 1,810,000 and 220,000, respectively (Mw/Mn of 8.2), which were much larger than the values corresponding to a commercially available cellulose (Mw = 68,300, Mn = 13,600, and Mw/Mn = 5.0, Wako Chemicals). In contrast, the Mw and Mn values of lignin were calculated to be 630 and 330, respectively. These low molecular-weight values were likely due to incomplete dissolution of lignin in THF, which prevented inclusion of high-molecular-weight lignin in the estimate of total lignin content.

A preliminary experiment was performed to determine the solubility of newspaper in the H_3PO_4 solvent. A mixture of newspaper (0.1 g) and 85% H_3PO_4 (1.8 g) was added to a glass container, rather than the electrolysis cell, to acquire a sufficient amount of sample for filtration and analysis. The mixture was heated at 125–175 °C for 30 min and then filtered; both filtrate and residue were collected. As shown in Fig. 2, the filtrate collected at 175 °C included $C_{14}H_{14}O_8Na$ and $C_5H_7O_3$, the structural formulas of which were determined from the parent and fragment ions. All components of the filtrates are summarized in Table S1. (Sodium ions probably came from the glass container.) Importantly, the amounts of residues at all temperature tested were less than 6 wt%, which decreased to 2.4 wt% at 175 °C. Therefore, a considerable amount of newspaper was decomposed to mono- and disaccharide derivatives and an aliphatic keto acid in the H_3PO_4 solvent at elevated temperatures.

3.2. Electrolysis of newspaper using Pt/C anode

As a control experiment, electrolysis of newspaper was performed using the Pt/C anode. Fig. 3(a) shows *I-V* curves for the electrolysis cell at temperatures between 100 and 175 °C. The current densities obtained without biomass fuels were less than 0.01 A cm^{-2} at a cell voltage of 1 V, as previously reported [14], which indicates that water present in the H_3PO_4 solvent is not electrolyzed under the present conditions. In contrast, the current densities obtained for newspaper were one or two orders of magnitude greater than those in the blank experiments, which became more significant as the temperature increased from 100 to 175 °C. A similar temperature effect was observed for electrolysis onset voltage: onset voltage was *ca.* 0.4 V at 100 °C, but

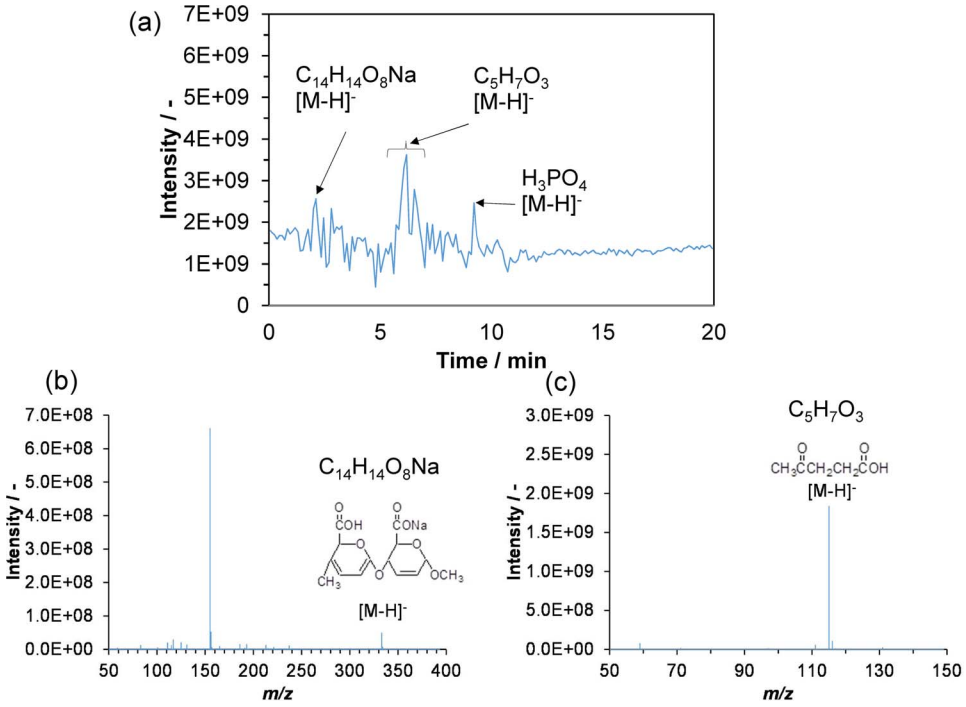

Fig. 2. LC/MS chromatograms of the filtrate obtained at 175 °C.

lowered to *ca.* 0.2 V at 175 °C. These temperature effects were attributed to the decomposition of cellulose and lignin to small molecules at elevated temperatures, which accelerated the anode reaction due to reactive carbonyl groups in the decomposition products. Interestingly, almost identical *I-V* curves were observed upon using unprinted newspaper fuel (Fig. S2), which indicates that the ink components did not significantly affect the electrolysis characteristics. Furthermore, the *I-V* values using the newspaper were somewhat lower than those using pure cellulose, but greater than those using pure lignin (Fig. S3), which reflects the cellulose-rich composition of the newspaper (Fig. 1(a)).

Fig. 3(b) shows the impedance spectra for the electrolysis cell at various temperatures. The impedance spectra recorded at 100 °C consisted of three impedance components: ohmic resistance, polarization resistance, and Warburg impedance related to diffusion processes in the electrode. When the temperature was raised, ohmic resistance remained almost unchanged, due to the low activation energy for proton conduction in the electrolyte [30,31]. In contrast, polarization and mass-transfer resistances decreased significantly with temperature, which

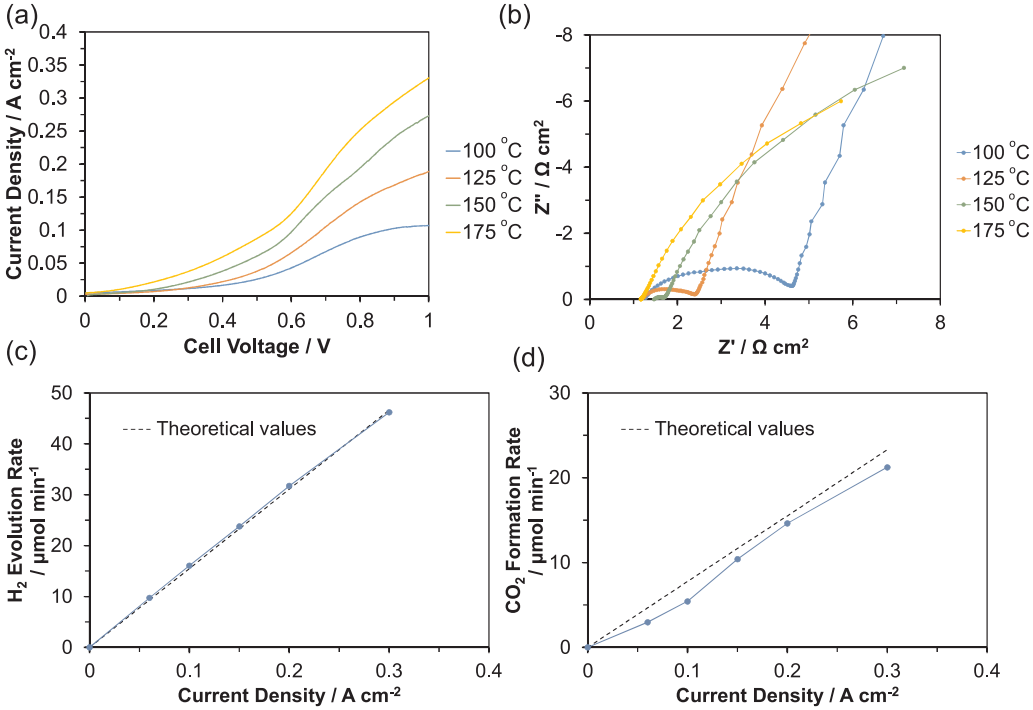

Fig. 3. Electrolysis characteristics of the batch cell using the Pt/C anode: (a) *I-V* curves between 100 and 175 °C and (b) impedance spectra between 100 and 175 °C. Evolution and formation rates of (c) H_2 and (d) CO_2, respectively, at 175 °C. Theoretical values are included for comparison.

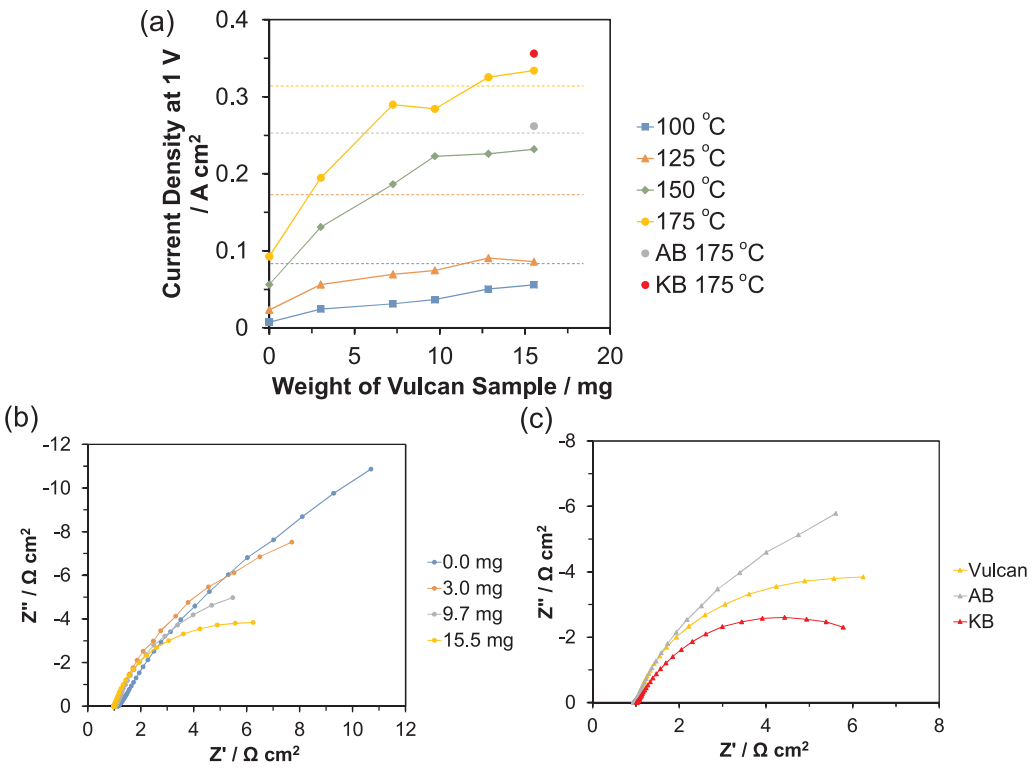

Fig. 4. Electrolysis characteristics of batch cells using various carbon anodes at temperatures between 100 and 175 °C: (a) current densities obtained at a cell voltage of 1 V as a function of Vulcan sample weight. Data for the Ketjen black (KB) and acetylene black (AB) samples (16 mg each) are also induced. Impedance spectra of (b) the Vulcan anode with different amounts at 175 °C and of (c) different carbon species at 175 °C.

improved the electrolysis characteristics upon an increase in temperature. The amounts of H_2 evolved at the cathode and of CO_2 formed at the anode were monitored at 175 °C in a current-density range of 0–0.3 A cm^{-2}, and were compared with the theoretical values calculated using Faraday's law. Based on Reactions (3) and (4), H_2 and CO_2 are assumed to be formed by two- and four-electron reactions, respectively, although the number of electrons (z) transferred per CO_2 molecule in Reaction (4) is exactly 4.38. For electrolysis with a constant current (I), the mole number (n) of H_2 or CO_2 formed per minute can be estimated by:

$$n = (I\ A \times 60\ second) / (z \times 96485\ C) \quad (6)$$

The current efficiencies, ratios of the actual rates to the theoretical values, were approximately 1.0 and 0.9 for H_2 evolution and CO_2 formation, respectively (Figs. 3(c) and (d)), which were comparable to the values obtained for pure cellulose or lignin [14].

3.3. Design of highly active carbon anode for newspaper oxidation reaction

Vulcan carbon black, the carbon support of the Pt/C electrode, was also investigated. Fig. 4(a) shows current densities obtained at a cell voltage of 1 V as a function of weight of the Vulcan sample at temperatures between 100 and 175 °C. One distinctive feature of the Vulcan anode was the large effect of sample weight and temperature on current density. This resulted in a current density recorded for 16 mg of Vulcan at 175 °C that was comparable to the value observed for the Pt/C anode under the same conditions (indicated by the yellow dotted line). These effects were attributed mainly to the reduction in mass-transfer resistance upon an increase in sample weight, which was further increased by a negligibly small polarization resistance at a temperature of 175 °C, as shown in Fig. 4(b). Data for Ketjen black and acetylene black (16 mg of each) are also included in Fig. 4(a). Current density was dependent on the carbon black species in the order: Ketjen black > Vulcan > acetylene black. This dependence was related closely to the difference in mass-transfer resistance among the carbon species, as shown in Fig. 4(c). One possible explanation for this relation is the correlation between mass-transfer resistance and the specific surface area of the carbon types: 1,216, 214, and 76 $m^2\ g^{-1}$ for Ketjen black, Vulcan, and acetylene black, respectively, indicating increases in the adsorption capacity for the decomposition products and in the active site volume for the anode reaction.

Acid functional groups are important in both the adsorption and reaction processes. Carboxyl groups enhance the wettability of the carbon surface and consequently increase adsorption capacity of the carbon [32,33]. Alternatively, the carbonyl groups act as redox active sites on the carbon surface [16,17]. Therefore, the Ketjen black sample was treated with HNO_3 at room temperature to form acid functional groups [22]. Current densities recorded at temperatures other than 100 °C reached a maximum at a treatment time of 20 h, and then decreased slightly (Fig. S4(a)); this was reflected by the mass-transfer resistance value of the oxygenated Ketjen black samples (Fig. S4(b)). To evaluate the effect of oxygenation on anode activity to enhance this effect, the Ketjen black sample treated for 47 h was used in subsequent experiments. The BET specific surface area of the carbon was nearly unchanged before and after acid treatment (Fig. 5(a)), as indicated by similar porosity among the samples: average micropore diameter 1.9 and 2.0 nm; mesopore diameter 5.9 and 6.2 nm; micropore volume 0.5 and 0.6 $cm^3\ g^{-1}$; mesopore volume 2.4 and 2.5 $cm^3\ g^{-1}$ (Fig. S5). In contrast, the XPS spectrum for the treated carbon contained more intense carbonylic C═O (287.8 eV) and carboxylic COO (288.9 eV) peaks [34], compared to those in the spectrum of the untreated carbon (Fig. 5(b)). These results imply that the carbon surface was partially oxygenated without structural deformation. Next, the sample was reduced by being subjected to 10% H_2 in an argon carrier at 800 °C for 5 h. The resulting carbon had a surface area comparable to that of the oxygenated carbon (Fig. 5(a)), as well as a similar micropore diameter (1.7 nm), mesopore diameter (7.1 nm), micropore volume (0.5 $cm^3\ g^{-1}$), and mesopore volume (2.6 $cm^3\ g^{-1}$) (Fig. S5). The intensity of the carboxylic COO peak was lower than that of the oxygenated carbon peak, although no significant difference in the intensity of the carbonylic C═O peak was seen between the two samples (Fig. 5(b)). Thus, the thermally unstable carboxyl groups apparently were removed mainly by the reduction treatment. Fig. 5(c) shows impedance spectra for electrolysis cells with the untreated, oxygenated,

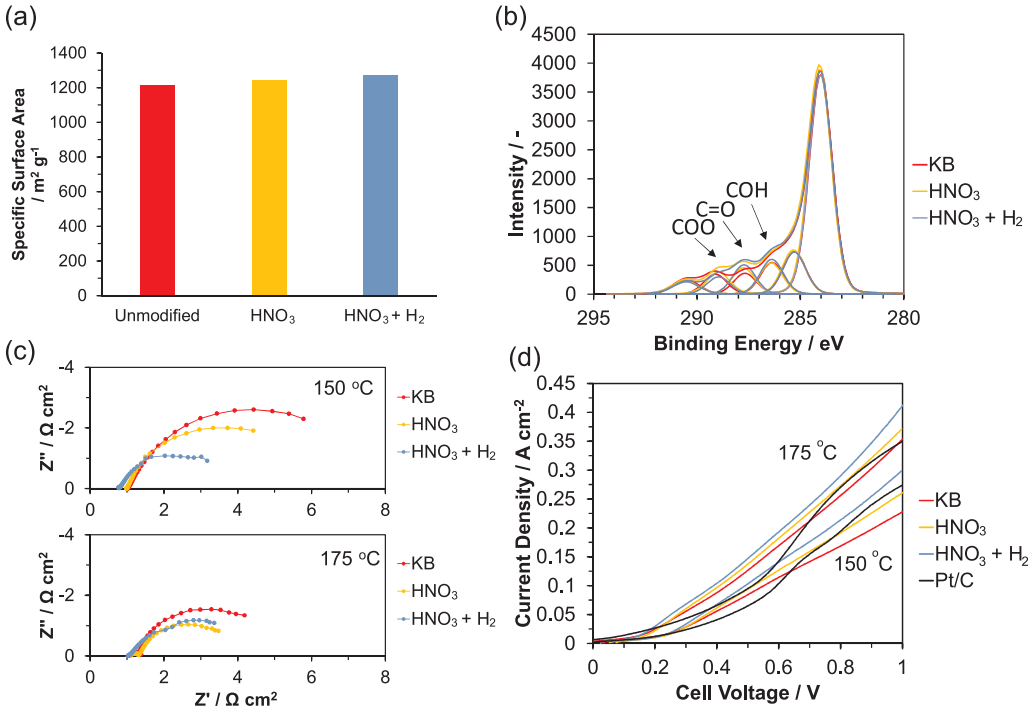

Fig. 5. Characterization of Ketjen black (KB) samples after HNO_3 treatment and H_2 reduction: (a) BET specific surface areas and (b) XPS spectra of C1s. (c) Impedance spectra and (d) *I-V* curves for electrolysis cells with the unmodified, oxygenated, and oxygenated and then reduced KB anodes at 150 and 175 °C.

and oxygenated and then reduced Ketjen black anodes. The mass-transfer resistance decreased significantly upon oxygenation and subsequent reduction. Fig. 5(d) shows *I-V* curves for the electrolysis cells with three carbon anodes at 150 and 175 °C. At both temperatures, current density at each cell voltage increased in the same order as the impedance. Notably, the optimized Ketjen black anode exhibited greater catalytic activity than that of the Pt/C anode at 150 and 175 °C; this was confirmed by the difference in impedance between these anodes (Fig. S6). Based on these results, the following scheme is proposed for the anode process: the transfer distance of reactants to the reaction sites was shortened by an increase in the active site density of the carbonyl groups, decreasing mass-transfer resistance of the Ketjen black anode. In contrast, the wettability of the carbon surface provided by the carboxyl groups was not strongly associated with the mass-transfer resistance of the Ketjen black anode.

The *I-V* curve obtained for the optimized Ketjen black anode (Fig. 5(d)) also showed that onset voltage of electrolysis was *ca.* 0.2 V at 175 °C, similar to that observed for the Pt/C anode under the same conditions (Fig. 3(a)). The impedance spectra were acquired at a temperature of 175 °C in a bias-voltage range of 0–0.6 V (Fig. S7). Very little difference in impedance was found between 0 and 0.1 V, above which an increase in bias voltage reduced the mass-transfer resistance of the cell, indicating that the electrode reactions began at bias voltages greater than 0.1 V, which correspond to the electrolysis onset voltage seen in the *I-V* curve.

3.4. Electrolysis of newspaper using optimized carbon anode

All experiments in this section were conducted galvanostatically at a temperature of 175 °C for both batch and flow methods. Fig. 6(a) shows MS spectra of H_2 and CO_2 during continuous electrolysis in the batch operation at various current densities, with an interval of 200 s at each current density. Constant quantities of H_2 and CO_2 were produced continuously at the cathode and anode, respectively, at each current density. The quantity of H_2 recorded at 0.3 A cm^{-2} agreed well with the theoretical value, while the quantity of CO_2 observed at this current density was smaller than the theoretical value. These characteristics were similar to those observed using the Pt/C anode, which suggests similarity in the reaction process between the two electrodes. Fig. 6(b) shows voltage-time curves for the electrolysis cell under the same conditions as in Fig. 6(a). Cell voltage increased almost linearly with time at each current density, due to a decrease in the amount of available fuel at the anode with time in the batch operation. Voltage-time curves obtained during longer electrolysis periods at 0.06, 0.10, and 0.15 A cm^{-2} are displayed in Fig. 6(c). The voltage-time curves possessed three common features compared to that of the blank experiment. First, plateau-like behavior in the voltage occurred beyond 1000 to 2000 s, which lengthened as current density decreased. Second, small voltage swells were observed at cell voltages between 1.25 and 1.50 V, due to electrolysis of water molecules in the H_3PO_4 solvent. Note that the concentration of water in the solvent was much less than the initial concentration (15%) because water molecules evaporated and were consumed in Reactions (3) and (4), as previously reported [12]. Third, the voltage increased rapidly due to depletion of both the fuel and water in the anode. The quantity of H_2 produced from the newspaper was calculated from the values for current and time before water electrolysis using Faraday's law. Results were 3.1, 2.5, and 2.2 mg for 0.06, 0.10, and 0.15 A cm^{-2}, respectively. These values were similar to the value of 2.4 mg calculated from the composition of the newspaper. Thus, 0.15–0.21 g of H_2 can be produced from 1 g of newspaper.

To better understand electrolysis characteristics, newspaper was electrolyzed using a flow process. Fig. 7(a) shows voltage-time curves for the electrolysis cell at various current densities. Compared to the results obtained in the batch process (Fig. 6(b)), the voltages were more plateau-like, and cell voltages were lower, due to a continuous supply of fuel to the anode, unlike the batch operation that involved capture of the fuel by the anode; therefore, this electrolysis cell stabilized the cell voltage and provided low mass-transfer resistance of the anode. Overall electrical resistance decreased to *ca.* 2.5 Ω cm^2, which was less than that obtained in the batch operation by about 1 Ω cm^2 (Fig. 5(c)). Fig. 7(b) shows the rates of H_2 evolved during continuous electrolysis under the same conditions shown in Fig. 7(a). H_2 was produced at a constant rate at all current densities tested, although some noise was

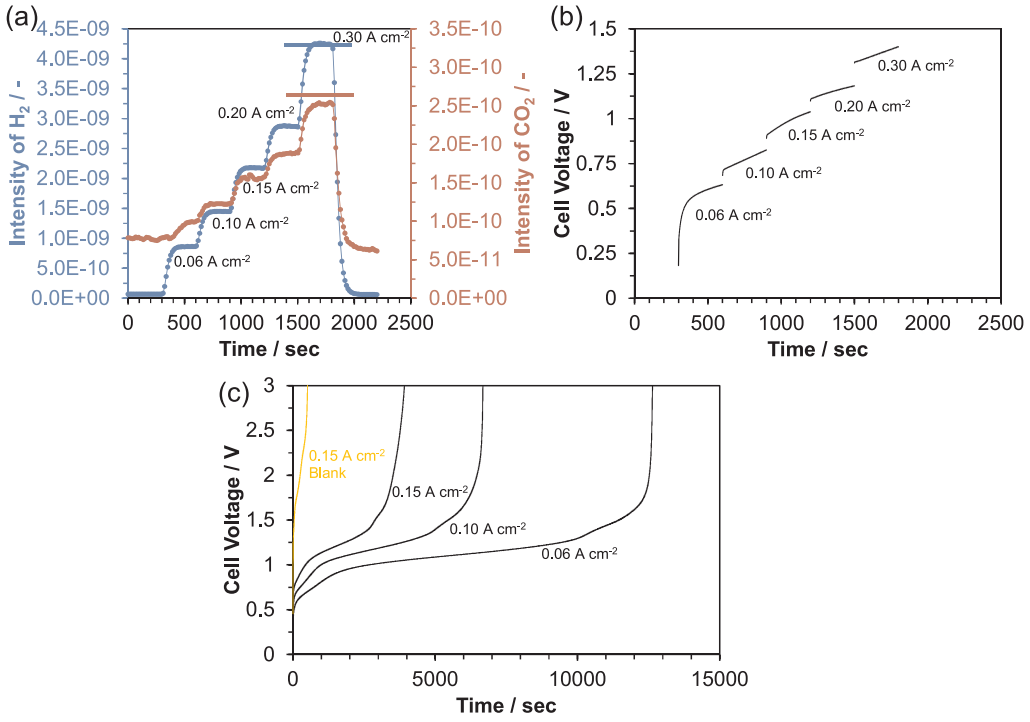

Fig. 6. Electrolysis characteristics of the batch cell using the optimized Ketjen black anode: (a) MS spectra for H_2 and CO_2 and (b) voltage-time curves during continuous electrolysis. (c) Voltage-time curves during longer electrolysis periods at various current densities.

present. Another important result is the agreement of H_2 evolution rates with the theoretical values (brown solid lines), similar to the results from the batch operation. The energy consumed for electrolysis was calculated by integrating the area under the voltage-time curve shown in Fig. 7(a), multiplying by the current, and then dividing by the volume of H_2 produced. The energy estimated at a current density of $0.15\,A\,cm^{-2}$ was $0.60\,kW\,h\ (Nm^3)^{-1}$. In addition, the power consumption of the two cartridge heaters was $0.67\,kW\,h\ (Nm^3)^{-1}$, where

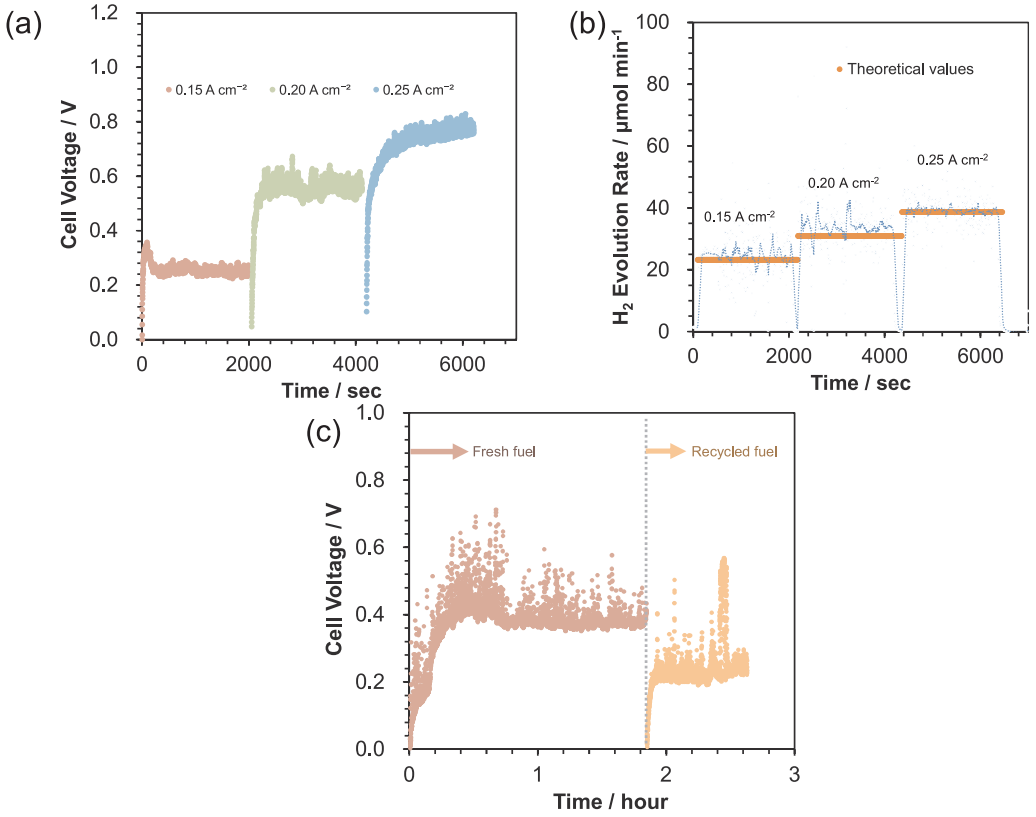

Fig. 7. Electrolysis characteristics of the flow cell using the optimized Ketjen black anode: (a) voltage-time curves and (b) H_2 evolution rate during continuous electrolysis at various current densities. (c) Voltage-time curves during longer electrolysis periods and during electrolysis of recycled fuel at $0.15\,A\,cm^{-2}$.

average voltage and current were 2.5 V per heater and 0.0084 A per heater, respectively. Accordingly, the total amount of electric energy was 1.27 kW h $(Nm^3)^{-1}$, which was less than that reported for ethanol electrolysis [*ca.* 2 kW h $(Nm^3)^{-1}$] [11]. Therefore, the present approach significantly reduces the amount of energy required for producing H_2. Attempts were made to clarify whether electrolysis could proceed without depleting the fuel and whether the H_3PO_4 could be recycled for subsequent electrolysis. Fig. 7(c) shows voltage-time curves during longer electrolysis periods at a current density of 0.15 A cm^{-2} and during electrolysis using recycled fuel at this current density. Plateau-like behavior was confirmed for 1 h 50 min (maximum time available for the apparatus used), which greatly exceeded depletion time of the fuel in the batch operation (Fig. 6(c)). Next, when the fuel collected at the outlet was reused for electrolysis, a new plateau appeared at a lower cell voltage. This low cell voltage was likely due to decomposed products that remain unreacted in the recycled fuel, leading to a decrease in the mass-transfer resistance of the anode upon reuse. Furthermore, the pH values estimated for the inlet and outlet solvents were 2.45 and 2.40, respectively, indicating that the H_3PO_4 concentration was virtually unchanged. These results indicate that the H_3PO_4 solvent could be recycled, even at a temperature of 175 °C. Note that the present electrolysis does not require any pretreatment outside the cell for newspaper fuel, which distinguishes it from other electrochemical techniques [35,36].

4. Conclusions

In conclusion, a method for electrolysis of waste newspaper directly to H_2 was developed using functionalized carbon anodes at intermediate temperatures. The newspaper was composed mainly of lignocellulose containing 69.2% cellulose and 11.8% lignin. These biomass components were decomposed to mono- and disaccharide derivatives and an aliphatic keto acid in H_3PO_4 solvent under conditions similar to those used for electrolysis. Electrolysis effectiveness was dependent on the carbon black species in the order: Ketjen black > Vulcan > acetylene black. The Ketjen black anode was modified by acid treatment, followed by reduction with H_2. This modification increased the quantity of carbonyl groups on the carbon surface and consequently decreased mass-transfer resistance, due to the shortened transfer distance between the reactants and reaction sites. As a result, the modified Ketjen black anode exhibited greater catalytic activity and smaller mass-transfer resistance for newspaper oxidation at temperatures of 150 and 175 °C, compared to those of a Pt/C anode. Newspaper electrolysis with this anode were characterized by a low onset voltage of *ca.* 0.2 V and high current efficiencies of approximately 1.0 and 0.9 for H_2 production and CO_2 formation, respectively. The yield of H_2 in a batch cell was 0.15–0.21 g per gram of newspaper. Constant quantities of H_2 were produced continuously in the current-density range of 0.15–0.25 A cm^{-2} at a temperature of 175 °C in a flow cell, where the cell voltage plateaued. This type of cell also continued to electrolyze newspaper by recycling the fuel collected at the outlet.

Acknowledgements

The authors would like to thank Dr. Miki Niwa (Professor Emeritus, Tottori University) for numerous useful discussions. This work was supported by Kakenhi Grants-in-Aid (Nos. 26000008 and 17H01895) from the Japan Society for the Promotion of Science (JSPS).

Appendix A. Supplementary data

Supplementary material related to this article can be found, in the online version, at doi:https://doi.org/10.1016/j.apcatb.2018.03.021.

References

[1] J.A. Turner, Sustainable hydrogen production, Science 305 (2004) 972–974.
[2] N. Savage, Fuel options: the ideal biofuel, Nature 474 (2011) S9–S11.
[3] C.L. Cheng, Y.C. Lo, K.S. Lee, D.J. Lee, C.Y. Lin, J.S. Chang, Biohydrogen production from lignocellulosic feedstock, Bioresour. Technol. 102 (2011) 8514–8523.
[4] L. Wang, C.L. Weller, D.D. Jones, M.A. Hanna, Contemporary issues in thermal gasification of biomass and its application to electricity and fuel production, Biomass Bioenergy 32 (2008) 573–581.
[5] V.S. Sikarwar, M. Zhao, P. Clough, J. Yao, X. Zhong, M.Z. Memon, N. Shah, E.J. Anthony, P.S. Fennell, An overview of advances in biomass gasification, Energy Environ. Sci. 9 (2016) 2939–2977.
[6] G. Kumar, P. Bakonyi, S. Periyasamy, S.H. Kim, N. Nemestóthy, K. Bélafi-Bakó, Lignocellulose biohydrogen: practical challenges and recent progress, Renew. Sustain. Energy Rev. 44 (2015) 728–737.
[7] M.A.Z. Bundhoo, R. Mohee, Inhibition of dark fermentative bio-hydrogen production: a review, Int. J. Hydrogen Energy 41 (2016) 6713–6733.
[8] S. Yun, S.T. Oyama, Correlations in palladium membranes for hydrogen separation: a review, J. Membr. Sci. 375 (2011) 28–45.
[9] J.L. Silveira, L.B. Braga, A.C.C. de Souza, J.S. Antunes, R. Zanzi, The benefits of ethanol use for hydrogen production in urban transportation, Renew. Sustain. Energy Rev. 13 (2009) 2525–2534.
[10] A. Caravaca, F.M. Sapountzi, A. Lucas-Consuegra, C. Molina-Mora, F. Dorado, J.L. Valverde, Electrochemical reforming of ethanol–water solutions for pure H_2 production in a PEM electrolysis cell, Int. J. Hydrogen Energy 37 (2012) 9504–9513.
[11] C. Lamy, T. Jaubert, S. Baranton, C. Coutanceau, Clean hydrogen generation through the electrocatalytic oxidation of ethanol in a proton exchange membrane electrolysis cell (PEMEC): effect of the nature and structure of the catalytic anode, J. Power Sources 245 (2014) 927–936.
[12] T. Hibino, K. Kobayashi, P. Lv, M. Nagao, S. Teranishi, T. Mori, An intermediate-temperature biomass fuel cell using wood sawdust and pulp directly as fuel, J. Electrochem. Soc. 164 (2017) F557–F563.
[13] T. Hibino, K. Kobayashi, P. Lv, M. Nagao, S. Teranishi, High performance anode for direct cellulosic biomass fuel cells operating at intermediate temperatures, Bull. Chem. Soc. Jpn. 90 (2017) 1017–1026.
[14] T. Hibino, K. Kobayashi, M. Nagao, S. Teranishi, Hydrogen production by direct lignin electrolysis at intermediate temperatures, ChemElectroChem 4 (2017) 3032–3036.
[15] A. Lotrič, M. Sekavčnik, A. Pohar, B. Likozar, S. Hočevar, Conceptual design of an integrated thermally self-sustained methanol steam reformer — High-temperature PEM fuel cell stack manportable power generator, Int. J. Hydrogen Energy 42 (2017) 16700–16713.
[16] A. Brunmark, E. Cadenas, Redox and addition chemistry of quinoid compounds and its biological implications, Free Radic. Biol. Med. 7 (1989) 435–477.
[17] J. Revenga, F. Rodriguez, J. Tijero, Study of the redox behavior of anthraquinone in aqueous medium, J. Electrochem. Soc. 141 (1994) 330–333.
[18] C.Y. Yin, M.K. Aroua, W.M.A.W. Daud, Review of modifications of activated carbon for enhancing contaminant uptakes from aqueous solutions, Separ. Purif. Technol. 52 (2007) 403–415.
[19] M.S. Shafeeyan, W.M.A.W. Daud, A. Houshmand, A. Shamiri, A review on surface modification of activated carbon for carbon dioxide adsorption, J. Analy. Appl. Pyrol. 89 (2010) 143–151.
[20] J. Rivera-Utrilla, M. Sánchez-Polo, V. Gómez-Serrano, P.M. Álvarez, M.C.M. Alvim-Ferraz, J.M. Dias, Activated carbon modifications to enhance its water treatment applications: an overview, J. Hazard. Mater. 187 (2011) 1–23.
[21] R.R.N. Marques, B.F. Machado, J.L. Faria, A.M.T. Silva, Carbon 48 (2010) 1515–1523.
[22] T. Hibino, K. Kobayashi, M. Nagao, S. Kawasaki, High-temperature supercapacitor with a proton-conducting metal pyrophosphate electrolyte, Sci. Rep. 5 (2015) 7903.
[23] H. Rabemanolontsoa, S. Ayada, Saka S, Quantitative method applicable for various biomass species to determine their chemical composition, Biomass Bioenergy 35 (2011) 4630–4635.
[24] K. Yoshihara, T. Kobayashi, T. Fujii, I. Akamatsu, A novel modification of Klason lignin quantitative method, Jpn. Tappi. 38 (1984) 466–475.
[25] K. Kurada, Mokuzai bunseki, Mokushitsu Kagaku Jikken Manual, Buneido shuppan, Tokyo, 2000 pp. 87–98.
[26] M.H. Entezari, Z.S. Al-Hoseini, Sono-sorption as a new method for the removal of methylene blue from aqueous solution, Ultrason. Sonochem. 14 (2007) 599–604.
[27] K. Iida, How technological innovations changed newsprint and its making process—Survey on technological developments in newsprint production in Japan (part IV), Jpn. TAPPI J. 63 (2009) 1214–1220.
[28] L. Fu, S.A. McCallum, J. Miao, C. Hart, G.J. Tudryn, F. Zhang, R.J. Linhardt, Rapid and accurate determination of the lignin content of lignocellulosic biomass by solid-state NMR, Fuel 141 (2015) 39–45.
[29] W.K. El-Zawawy, M.M. Ibrahim, Y.R. Abdel-Fattah, N.A. Soliman, M.M. Mahmoud, Laboratory investigation of ethanol production from agricultural residues, 18th European Biomass Conference and Exhibition, Lyon, France, 2010, pp. 1746–1752.
[30] K. Scott, C. Xu, X. Wu, Intermediate temperature proton-conducting membrane electrolytes for fuel cells, Wiley Interdiscip. Rev. Energy Environ. 3 (2014) 24–41.
[31] O. Paschos, J. Kunze, U. Stimming, F. Maglia, A review on phosphate based, solid state, protonic conductors for intermediate temperature fuel cells, J. Phys. Condens. Matter 23 (2011) 234110.
[32] B. Sun, M. Skyllas-Kazacos, Chemical modification of graphite electrode materials for vanadium redox flow battery application—part II. Acid treatments, Electrochim.

Acta 37 (1992) 1253–1260.
[33] W. Li, J. Liu, C. Yan, Reduced graphene oxide with tunable C/O ratio and its activity towards vanadium redox pairs for an all vanadium redox flow battery, Carbon 55 (2013) 313–320.
[34] A.P. Terzyk, The influence of activated carbon surface chemical composition on the adsorption of acetaminophen (paracetamol) in vitro: Part II. TG, FTIR, and XPS analysis of carbons and the temperature dependence of adsorption kinetics at the neutral pH, Colloids Surf. A: Physicochem. Eng. Asp. 177 (2001) 23–45.
[35] X. Du, W. Liu, Z. Zhang, A. Mulyadi, A. Brittain, J. Gong, Y. Deng, Low-energy catalytic electrolysis for simultaneous hydrogen evolution and lignin depolymerization, ChemSusChem 10 (2017) 847–854.
[36] F. Xu, H. Li, Y. Liu, Q. Jing, Advanced redox flow fuel cell using ferric chloride as main catalyst for complete conversion from carbohydrates to electricity, Sci. Rep. 7 (2017) 5142.